HHS Public Access

Author manuscript

Sci Immunol. Author manuscript; available in PMC 2017 July 11.

Published in final edited form as:

Sci Immunol. 2017 March ; 2(9): . doi:10.1126/sciimmunol.aaj1996.

Up-regulation of LFA-1 allows liver-resident memory T cells to patrol and remain in the hepatic sinusoids

H. A. McNamara[1], **Y. Cai**[1], **M. V. Wagle**[1], **Y. Sontani**[1], **C. M. Roots**[1], **L. A. Miosge**[1], **J. H. O'Connor**[1], **H. J. Sutton**[1], **V. V. Ganusov**[2], **W. R. Heath**[3], **P. Bertolino**[4], **C. G. Goodnow**[1,5], **I. A. Parish**[1], **A. Enders**[1], and **I. A. Cockburn**[*,1]

[1]Department of Immunology and Infectious Disease, John Curtin School of Medical Research, The Australian National University, Canberra, ACT 2602, Australia

[2]Department of Microbiology, University of Tennessee, Knoxville, Tennessee, United States of America

[3]Department of Microbiology and Immunology, The Peter Doherty Institute, University of Melbourne, Parkville, VIC 3010, Australia

[4]Liver Immunology Program, Centenary Institute and AW Morrow Gastroenterology and Liver Centre, University of Sydney and Royal Prince Alfred Hospital, Locked Bag No. 6, Sydney, NSW 2042, Australia

[5]Immunogenomics Laboratory, Garvan Institute of Medical Research, Darlinghurst, Sydney, NSW 2010, Australia

Abstract

Liver-resident CD8+ T cells are highly motile cells that patrol the vasculature and provide protection against liver pathogens. A key question is: how can these liver CD8+ T cells be simultaneously present in the circulation and tissue-resident? Because liver-resident T cells do not express CD103 - a key integrin for T cell residence in epithelial tissues - we investigated other candidate adhesion molecules. Using intra-vital imaging we found that CD8+ T cell patrolling in the hepatic sinusoids is dependent upon LFA-1-ICAM-1 interactions. Interestingly, liver-resident CD8+ T cells up-regulate LFA-1 compared to effector-memory cells, presumably to facilitate this behavior. Finally, we found that LFA-1 deficient CD8+ T cells failed to form substantial liver-resident memory populations following Plasmodium or LCMV immunization. Collectively, our results demonstrate that it is adhesion through LFA-1 that allows liver-resident memory CD8+ T cells to patrol and remain in the hepatic sinusoids.

[*]To whom correspondence should be addressed: ian.cockburn@anu.edu.au.

Author Contributions: Study conception and design: HAM; PB; WRH; IAP; CGG; AE, IC and IAC. Acquisition of data: HAM; YC; MW; YS; CMR; LM; HJS; IAP and IAC. Analysis and interpretation of data: HAM, VVG, LM, AE and IAC. Drafting of manuscript: HAM and IAC. Critical revision: WRH, PB, IAP and AE.

Competing interests: The authors declare no competing interests.

Introduction

$CD8^+$ T cells play critical roles in protection against infectious diseases and cancers. One problem that T cells must overcome is that the number of infected cells can represent a tiny fraction of cells in the body. To achieve efficient tissue surveillance, specialized populations of $CD8^+$ T cells that patrol different niches develop after priming. The first populations to be defined, based on the expression of CD62L and CCR7, were central and effector memory $CD8^+$ T cells (1). More recently populations of tissue resident memory (T_{RM}) cells have been identified in numerous tissues - especially barrier tissues - such as the skin, lung, gut and female reproductive tract (2-6). Such cells are strictly defined by their inability to recirculate from their tissue of residence, though they are frequently identified by the expression of CD69 and the integrin CD103 (2, 3, 6). Intra-vital imaging studies have revealed that $CD8^+$ T_{RM} cells in the skin are largely sessile cells that may act as sentinels against invading pathogens (7). This is consistent with the finding that these cells function as the first line of defense in peripheral tissues, able to recruit other cells to the immune response (8).

Given that the liver is the target organ of important pathogens including Hepatitis B Virus, Hepatitis C Virus and *Plasmodium*, several recent studies have begun to characterize T_{RM} cells in this organ (5, 9, 10). Although previously the liver was thought of as a “graveyard” for $CD8^+$ T cells, it is now clear that it harbors large numbers of memory $CD8^+$ T cells capable of protecting against pathogen challenge (11, 12). We have recently shown that the formation of robust $CD69^+$ $CD8^+$ T cell populations is essential for effective protection against *Plasmodium* (malaria) liver stages (9). Based on parabiosis studies these $CD69^+$ cells in the liver have been defined as a resident population that does not recirculate within 2-3 months (5, 9). Liver T_{RM} cells also share with epithelial T_{RM} cells a common gene expression signature dependent on the expression of the transcription factors Hobit and Blimp1 (9, 10). However, liver $CD8^+$ T cells have some distinct features compared to epithelial T_{RM} cells: notably most liver T_{RM} cells are present in the circulation as revealed by in vivo antibody labeling experiments (5, 9). Intra-vital imaging has further shown that liver T_{RM} display motile patrolling behavior in the hepatic sinusoids (9).

A critical question therefore is: what are the molecular interactions that retain $CD8^+$ T cells in the liver and facilitate their patrolling behavior? Interestingly liver T_{RM} cells do not express high levels of CD103 (9, 10), an integrin that is required for T_{RM}s to be retained in many epithelial tissues (13). One the other hand, a variety of other adhesion molecules have been implicated in the migration of $CD8^+$ T cells to the liver. The initial trapping of $CD8^+$ T cells in the liver appears to be mediated by interactions between $CD8^+$ T cells and platelets bound to the endothelium via CD44, rather than selectin-mediated rolling interactions (14). Some studies have suggested that ICAM-1 is required for the retention of naive and activated $CD8^+$ T cells in the liver but only in the presence of antigen (15, 16). Intriguingly, while the ICAM-1 ligand LFA-1 has been found to be critical for NKT cell retention in the liver (17, 18), this canonical adhesion molecule has been regarded as dispensable for the intrahepatic retention of activated $CD8^+$ T cells (14, 17).

Here we investigated the roles of a range of adhesion molecules in the intrahepatic migration of effector and memory $CD8^+$ T cells using intra-vital imaging. We found that, surprisingly, ICAM-1-LFA-1 interactions are indeed important for the movement of activated $CD8^+$ T cells in the liver. Further analysis revealed that LFA-1 is highly expressed specifically on liver T_{RM} cells and that its absence results in their inability to establish residence in the liver. Our data thus reveal an unexpected role for the adhesion molecule LFA-1, rather than CD103, in the retention of liver T_{RM} cells and highlight the distinct adhesion molecule requirements for memory T cells that patrol vascular, rather than barrier, tissues.

Results

Activated $CD8^+$ T cells use LFA-1:ICAM-1 interactions to patrol the liver

Previous studies have shown that $CD8^+$ T cell migrate in the hepatic sinusoids with a characteristic patrolling behavior that facilitates their ability to scan the liver and find pathogens such as *Plasmodium* and Hepatitis B virus (14, 19). We used antibody blockade to investigate the roles of ICAM-1, VCAM-1, and CD44 on the patrolling behavior of transferred in vitro activated $CD8^+$ T cells. These molecules have been proposed to have roles in the intrahepatic accumulation of $CD8^+$ T cells, though with the exception of CD44, their roles in migratory behavior within the liver have not been studied (14, 16). We also transferred cells to β2 microglobulin-deficient recipients to examine the role of MHC Class I interactions which have also been suggested to be important for $CD8^+$ T cells adhesion in the liver (20). We subsequently examined the migration of the activated $CD8^+$ T cells in the liver by time-lapse multi-photon microscopy (Movie S1). Surprisingly only ICAM-1 blockade had any effect on $CD8^+$ T cell movement, with cells in treated mice moving more slowly and spending more time arrested than cells in control mice (Figure 1A-B) suggesting that ICAM-1 and its ligands might be important for $CD8^+$ T cell patrolling of the liver. In contrast antibodies to other adhesion molecules as well as rat IgG2b isotype control antibodies had no effect on migration of $CD8^+$ T cells (Figure S1). The reduction in crawling behavior seen in anti-ICAM-1 treated mice is consistent with previous in vitro studies which show that ICAM-1 is required for the crawling motility of lymphocytes as well as their adhesion (21).

Given that ICAM-1 is highly expressed on the surface of liver sinusoidal endothelial cells and hepatocytes (14, 20), we hypothesized that T cells were crawling on these surfaces using the integrin LFA-1 that is highly expressed on $CD8^+$ T cells. LFA-1 is composed of integrin alpha-L (ITGAL; CD11a) combined with integrin beta-2 (CD18). To further investigate a possible role of LFA-1 in T cell migration in the liver we used a mouse line carrying a Cys77Phe mutation caused by a G>T change in Exon 3 of the *Itgal* gene (Chromosome 7, position 127299608). This mutation causes a complete lack of ITGAL on the cell surface (Figure S2A), accordingly we designate them $Itgal^{/-}$ for simplicity. It is likely that Cys77 forms disulphide bonds and that the mutation destabilizes the integrin structure. These mice were identified from an ENU mutagenesis screen for immune phenotypes in the blood (22) as they have an elevated proportion of NKT cells in the blood (Figure S2B). This may be explained by the fact that LFA-1 has been shown to be important for the intrahepatic retention of NKT cells (18). Closer analysis of our $Itgal^{/-}$ mice revealed that they also have

elevated CD8$^+$ T cells in the blood, particularly CD44^{hi} activated CD8$^+$ T cells (Figure S2B).

To investigate the effect of loss of ITGAL on CD8$^+$ T cell migration in the liver we activated *Itgal*$^{-/-}$ OT-I cells in vitro and co-transferred them to mice with similarly activated but differentially labeled WT OT-I cells. Migration in the liver was then assessed by multi-photon microscopy (Movie S2; Figure 1C). In agreement with our ICAM-1 blockade data, *Itgal*$^{-/-}$ cells did not display patrolling behavior, rather they spent large amounts of time arrested and moved with slower average speeds than WT cells (Figure 1D). Importantly the *Itgal*$^{-/-}$ and WT cells showed similar expression of activation markers and other β2 integrins, suggesting that the reduced migration was not due to inadequate priming of *Itgal*$^{-/-}$ cells resulting in the expression of different adhesion molecules (Figure S3). We further used flow cytometry to quantify the accumulation of cells in the liver and other organs in mice that received equal numbers of WT and *Itgal*$^{-/-}$ cells. In the liver and lungs *Itgal*$^{-/-}$ cells constituted <20% of the cells recovered from these mice; in contrast *Itgal*$^{-/-}$ cells formed the major proportion of cells recovered from the spleen, blood and lymph nodes (Figure 1E and F). One hypothesis is that the spleen and lymph nodes act as a sink for the *Itgal*$^{-/-}$ cells, however our intra-vital imaging data (Figure 1B and C), and our finding that there are also elevated numbers of *Itgal*$^{-/-}$ cells circulating in the blood suggest this is not the case. Rather our data suggest that LFA-1 is important for the retention of activated CD8$^+$ T cells in the liver and lungs.

LFA-1 is required for efficient CD8$^+$ T cell mediated protection against malaria

We next wanted to determine if the lack of patrolling cells in the liver would affect protection against the *Plasmodium* parasite. While CD8$^+$ T cells are capable of killing parasites in the liver (19), it is not known whether the cells conferring protection are those circulating in the blood or those migrating in the sinusoids. Given the results of the previous experiment, in which the *Itgal*$^{-/-}$ cells are enriched in the blood and WT cells are enriched in the liver, we were able to test this by transferring activated *Itgal*$^{-/-}$ or WT OT-I cells to mice prior to challenge with *P. berghei* CS^{5M} parasites that express the SIINFEKL epitope within the immunodominant circumsporozoite (CS) protein (23). Strikingly we found that the parasite burden was significantly greater in mice that received the *Itgal*$^{-/-}$ cells rather than WT cells (Figure 2A). While a component of this impaired protection by *Itgal*$^{-/-}$ cells may be attributed to a defect in cytotoxicity (Figure 2B) we also observed by intra-vital microscopy that WT OT-I cells were better able to associate with and cluster around *P. berghei* CS^{5M} parasite than *Itgal*$^{-/-}$ OT-I cells (Figure 2 C and D). Thus our data are consistent with the hypothesis that LFA-1-mediated patrolling of the liver is required for efficient immune-surveillance, though we cannot exclude the possibility that LFA-1 is also important for CD8$^+$ T cell killing of infected cells.

Memory T cells in the liver adopt a characteristic patrolling behavior in the hepatic sinusoids

We next wanted to determine if the migratory behavior we observed in in vitro activated cells reflects that of in vivo primed cells. Accordingly, we immunized mice that had received naïve GFP$^+$ OT-I cells with *P. berghei* CS^{5M} sporozoites. The livers of mice were then

imaged at effector (1 week) and memory (4 weeks) time-points post-immunization (Figure 3A and B and Movies S3 and S4). At effector time-points the behavior of donor T cells in the liver was different to that observed with in vitro activated cells. Notably, there were many rounded up cells and cells moving with the blood flow. To capture these rapidly-moving cells we modified our imaging protocol and made high frame-rate movies (3 frames/second) using the resonant scanner on our microscope. Mathematically we were then able to distinguish three migratory phenotypes among the GFP^+ cells using the parameters of cell speed and polarity (Figure 3C). The first population we designated "flowing" cells, these cells moved rapidly (>25 μm/min; median = 208 μm/min) in the blood though sometimes they briefly arrested on the walls of the sinusoids. Among the non-flowing cells moving at <25 μm/s we observed a population of "rounded" cells which we formally defined as having polarity <1.5; these cells were often arrested but sometimes detached (median speed = 5.8 μm/min). Finally we were able to observe some "patrolling" cells that we defined by their higher polarity (>1.5). Overall these cells moved similarly to in vitro activated cells, though they had a higher median speed (9.5 μm/s). At the memory time-point a strikingly different picture was seen, with a substantial increase in the number of patrolling cells which increased from <5% of cells 1 week post-immunization to >50% of the total cells at 4 weeks post-immunization (Figure 3D). We further found that ICAM-1 blockade reduced the speed and increased the arrest coefficient of memory $CD8^+$ T cells in the liver (Figure 3E), suggesting that these cells, like in vitro activated effectors, use LFA-1:ICAM-1 interactions for their patrolling behavior.

Liver resident memory $CD8^+$ T cells express exceptionally high levels of LFA-1

Given that LFA-1 was found to be important for migration of in vitro activated $CD8^+$ T cells in the liver we speculated that the formation of a patrolling memory population in the liver might be associated with an increase in the expression of LFA-1 (ITGAL; CD11a) on $CD8^+$ T cells. We examined the phenotypes of OT-I cells in the spleen, lymph node and livers of mice at 1, 2 and 4 weeks post-immunization with *P. berghei* CS^{5M} sporozoites (Figure 4A). Naïve cells expressed low levels of LFA-1 that increased upon priming (Figure S4). CD11a was expressed at intermediate levels on activated $CD8^+$ T cells in the spleen at all time-points, however, at 2 weeks and 4 weeks post-immunization we observed a distinct population of $CD11a^{hi}$ cells in the liver (Figure 4A and 4B; Figure S4). Importantly this population did not appear to be present in the lymph nodes and spleen- which is consistent with our previous data (Figure 1E-F) – suggesting that LFA-1 is dispensable for homing to these organs.

We were further interested in knowing the broader phenotype of the $CD11a^{hi}$ population, particularly if they might correspond to liver T_{RM} $CD8^+$ T cells. We found that, indeed, $CD11a^{hi}$ cells were almost exclusively $CD69^+$ $KLRG1^-CXCR3^+$ (Figure 5A and B), a typical profile for liver T_{RM} cells (9, 10). We also found that the $CD11a^{hi}$ cells in the liver did not express high levels of CD103 (Figure 5B), while IV injection of FITC-labeled anti-CD8a antibody revealed these cells to be in the circulation (Figure S5A) which is also in agreement with previous descriptions of liver T_{RM} cells (5, 9, 10). To determine if this $CD11a^{hi}$ population is unique to the liver or may be seen in other tissues, we examined the spleen, lymph node, blood, skin and lungs of mice immunized with sporozoites. While we

were unable to detect antigen specific cells in the skin of sporozoite immunized mice, we were able to detect CD11a^{hi} CD69^{+} cells in the lungs of immunized mice (Figure 5C and D). However these lung CD11^{hi} cells were unlikely to be T_{RM} cells because lung T_{RM} cells express CD103 and are IVAb^{-} (6, 24) whereas the CD11^{hi} cells we observed were CD103^{-} and IVAb^{+} (Figure S5).

To determine whether the elevated expression of LFA-1 was specific to *Plasmodium*, we also examined CD11a expression on NP396 Tetramer^{+} cells following intra-peritoneal infection with LCMV Armstrong. Similar to our results with sporozoites we identified a CD11a^{hi} population in the liver that corresponded to the previously defined liver T_{RM} populations being CD69^{+} CD103^{-}KLRG1^{-} (Figure S6 A-C). We also identified a similar population of CD11a^{hi}CD69^{+}KLRG1^{-}cells in the lung after LCMV infection (Figure S6D). While in this case a modest proportion (~20%) of Tetramer^{+} cells were IVAb^{-} we did not detect any appreciable CD103 expression (Figure S6D), which is in agreement with previous observations that intra-peritoneal LCMV infection does not induce lung T_{RM} cells (25, 26). Independently, a distinct population of CD11a^{hi} cells in the liver has been observed previously following Vesicular Stomatitis Virus infection (27), though this observation was not followed up. Finally, we analyzed NKT cells as the other liver resident lymphocyte subset and found that NKT cells also have an identical CD11a^{hi} CD69^{+} KLRG1^{-} phenotype to liver T_{RM} cells (Figure S7).

LFA-1 is required for the retention of T_{RM} cells in the liver

To determine if LFA-1 is required for the intrahepatic retention of CD8^{+} T cells we first made mixed bone marrow chimeras containing CD45.2^{+} *Itgal*$^{-/-}$ cells mixed with CD45.1^{+} WT cells as well as control chimeras reconstituted with equal numbers of CD45.2^{+} and CD45.1^{+} WT cells. The contributions of *Itgal*$^{-/-}$ cells to the CD8^{+} T cell population were analysed in the spleen, lung and liver (Figure S8A). *Itgal*$^{-/-}$ CD8^{+} T cells migrated normally to the spleen but did not accumulate efficiently in either the lung or the liver, though the overall defect was only just significant in the liver (Figure S8B and C). Specific analysis of the contribution of *Itgal*$^{-/-}$ cells to the CD69^{+} and CD69^{-} liver cell populations (Figure S9A) revealed that the intrahepatic CD69^{+} subset came almost entirely from the WT cells (Figure S9B and C), indicating that ITGAL is required for its residency. In contrast, when we examined CD69^{-} CD8^{+} T cells in the liver we found that these were not dependent on ITGAL for retention in the liver (Figure S9B and C). A similar analysis of the lung CD69^{+} and CD69^{-} cell populations revealed that, in contrast to the liver, ITGAL is critical for the accumulation of both these populations in the lung (Figure S9D-F).

To determine if LFA-1 is required for the formation of antigen-specific liver T_{RM} cell populations after immunization we co-transferred GFP^{+} *Itgal*$^{-/-}$ and WT CD45.1^{+} OT-I cells to CD45.2^{+} mice prior to immunization with *P. berghei* CS^{5M} sporozoites (Figure 7A). At 1 week post-infection we observed that the WT cells outnumbered the *Itgal*$^{-/-}$ cells in both the liver and spleen by around 30:1 (Figure 7B), a result consistent with the priming defect previously reported for *Itgal*$^{-/-}$ cells (28). However, while this ratio remained constant at 4 weeks post-immunization in the spleen, in the liver, the *Itgal*$^{-/-}$ cells were now outnumbered

by around 60:1 suggesting these LFA-1-deficient cells have a specific defect in forming memory populations in this organ (Figure 7C).

Examination of the phenotypes of the cells revealed that the difference between the spleen and liver was largely driven by the relative proportions of $CD69^{+}KLRG1^{-}$ (T_{RM}) cells (Figure 7D). This population typically made up ~30% of the WT OT-I cells in the liver, but accounted for only ~10% of the *Itgal*$^{-/-}$ cells in the same mouse (Figure 7E). Interestingly, these cells may not be lost altogether but may enter the general circulation as in the spleen the situation was reversed with a higher proportion of T_{RM} phenotype cells among the *Itgal*$^{-/-}$ OT-I cells compared to the WT OT-I cells (Figure 7E). As a result of this the ratio of WT to *Itgal*$^{-/-}$ OT-I T_{RM} cells was 120:1 in the livers of immunized mice but only by 8:1 in the spleens (Figure 7F). Nonetheless the ratio of *Itgal*$^{-/-}$ to WT non-T_{RM} cells was still significantly lower in the liver compared to the spleen, suggesting that activated non-T_{RM} cells may still use ITGAL to accumulate in the liver.

We also investigated the ratio of *Itgal*$^{-/-}$ to WT OT-I cells in other organs in this experiment (Figure 7G). In agreement with our bone marrow chimera data, lung OT-I cells had an even stronger requirement for ITGAL than liver OT-I cells, with *Itgal*$^{-/-}$ cells being outnumbered by around 120:1 by WT cells. In contrast in the lymph nodes, *Itgal*$^{-/-}$ cells were only outnumbered around 8:1 by WT OT-I cells. This suggests that some *Itgal*$^{-/-}$ cells may accumulate in lymph nodes, though the proportion of OT-I cells in the lymph nodes was very small (Figure S5).

Finally we were concerned that our data might be biased by the poor priming of the LFA-1 deficient cells by *Plasmodium*, especially in a competitive environment. Accordingly we infected *Itgal*$^{-/-}$ mice and their WT littermates with LCMV-Armstrong and measured the formation of antigen specific T cell responses using NP396 tetramers. In this infection model there was no detectable defect in priming in the *Itgal*-/- mice as similar percentages of $Tetramer^{+}$ cells were seen in the blood 1 week post immunization (Figure 7A). Moreover, 4 weeks post-immunization there were similar proportions and numbers of $Tetramer^{+}$ cells between the *Itgal*$^{-/-}$ and littermate mice in both the spleen and liver (Figure 7 B and C). However while robust populations of antigen-specific $CD69^{+}$ $KLRG1^{lo}$ cells were formed in livers of littermate control mice, few were seen in *Itgal*$^{-/-}$ mice (Figure 7 D and E). Similar to our results with *Plasmodium* immunization there was a ~2-fold increase in the average numbers of $CD69^{+}$ $KLRG1^{+}$ cells in the spleens of *Itgal*$^{-/-}$ compared to littermates suggesting that these cells may accumulate in secondary lymphoid organs if they are unable to be retained in the liver, though this did not reach statistical significance when correction was made for multiple comparisons. Collectively these data from our bone marrow chimeras and 2 distinct models of infection suggest that LFA-1 is critically required for the retention of T_{RM} cells in the liver.

Discussion

Several recent papers have identified populations of tissue resident $CD69^{+}$ antigen specific memory cells in the liver that patrol the sinusoids (5, 9, 10). A critical question then is how can an intra-vascular population in the circulation also be tissue resident? Here we show a

critical role for ITGAL - and by extension the integrin LFA-1 - in the migration of activated $CD8^+$ T cells in the liver. We further show that LFA-1 is required for the retention of T_{RM} cells in the liver. It is possible that these cells might occasionally exit the liver if they were to enter the hepatic venules, though it may be that these cells rapidly recirculate back to the liver due to the elevated expression of ICAM-1 in these tissues and the slow blood flow within this organ (14, 20). Overall though, our data support the hypothesis that it is the expression of high levels of LFA-1 on the surface of this cell subset that allows them to remain in the liver and patrol the hepatic sinusoids.

Our data further suggest that T_{RM} populations in different tissues have different adhesion molecule requirements for tissue retention. In agreement with previous reports we do not detect high levels of the integrin CD103 on the surface of our $CD11a^{hi}$ liver T_{RM} cells (5, 10). CD103 is highly expressed on epithelial T_{RM} cells such as those found in the skin and the gut and has been shown to be required for T cell residence in the skin (2, 3, 13). Its expression appears to be induced, even in vitro, by TGF-β signaling (29). In vivo the level of CD103 expression increases progressively during skin T_{RM} development as they migrate to the epidermis (30). However while CD103 may be critical for the residence of T_{RM} cell populations in various epithelia it is presumably dispensable for T_{RM} populations that may in fact remain exposed to the circulation. Interestingly TGF-β signaling has previously been shown to down-regulate LFA-1 expression suggesting that these integrins may be reciprocally regulated (31, 32).

Despite ICAM-1/LFA-1 interactions being considered canonical in the leukocyte adhesion cascade, their role in liver residence has been unclear. While ICAM-1 has been suggested to have a role in the retention of naïve and activated cells in the liver (16, 20, 33), antibody blockade with α-LFA-1 antibodies was not found to inhibit the accumulation of activated $CD8^+$ T cells in the liver (14). Moreover, LFA-1 deficient mice do not possess abnormal numbers of conventional T cells in the liver (17). Our data resolve many of these contradictory observations. As with previous studies we did not see any effect of antibody blockade on retention of activated effector cells to the liver, only a defect in migration. Our data also explain why previous studies missed a role of LFA-1 in $CD8^+$ T cell migration to the liver, as LFA-1 is only absolutely required for the retention of the T_{RM} phenotype cells, while other $CD8^+$ T cells which are non-resident can transiently associate with the liver in the absence of LFA-1. Thus previous studies of bulk $CD8^+$ T cell populations were unable to detect the role of LFA-1 in this recently identified cell type.

Although our studies have focused on the role of LFA-1 in $CD8^+$ T cell accumulation in the liver we also find that this integrin is important for $CD8^+$ T cell retention in the lung. We identified a population of cells in the lung that was $CD11a^{hi}$, which like the corresponding population in the liver were $CD69^+$ and KLRG1-. However our $CD11a^{hi}$ $CD69^+$ cells are unlikely to be lung T_{RM} cells as lung T_{RM} cells are typically IV Ab^- and $CD103^+$ (6, 24). The absence of lung T_{RM} cells is not unexpected as *Plasmodium* does not infect the lung, while LCMV only forms significant lung T_{RM} populations after intra-tracheal infection (25). In contrast to the liver, in the lung both $CD69^+$ and $CD69^-$ $CD8^+$ T cells had a strong requirement for LFA-1 to be retained. This highlights again the different adhesion molecule requirements among diverse populations of $CD8^+$ T cells in different organs. Previous

studies have shown that LFA-1 is required for the retention of early effector cells in the lung (34), while another study has shown that LFA-1 is required for memory cell entry to the lung airways (35). Our results extend these previous results in showing an important role for LFA-1 for the retention of vascular $CD8^+$ T cell populations (as opposed to just those in the airways) at memory time-points. Interestingly, while liver sinusoids are characterized by slow blood-flow, in the lung the flow is faster and cells experience more sheer stress (36). Thus, LFA-1 may be universally required among $CD8^+$ T cell populations in the lung to allow even transient associations with the endothelium.

In summary we have discovered a previously unappreciated role for LFA-1 in the retention of $CD8^+$ T cells in the liver and for the movement of these T cells within hepatic sinusoids. This motility is what appears to be important for the efficient surveillance of the liver and the identification of infected cells (9). Crucially, because of the potential ability of the liver T_{RM} cells to enter the circulation directly, the mechanism of retention in the liver appears different to that described for epithelial or mucosal T_{RM} cells. Overall, our data suggest that the nature of tissue resident $CD8^+$ T cell populations may be even more diverse and complex than has previously been suggested.

Materials and Methods

Details of standard immunological methods used in this study are given in the supplemental materials and methods.

Study Design

The initial aim of the study was to determine the molecules involved in CD8+ T cell migration in the liver. Accordingly experiments were performed in which we blocked candidate adhesion molecules and measured motility by intra-vital imaging (Figure 1). As the *n* for these experiments was determined by the number of cells each mouse was considered an experimental repeat. No randomization or blinding was performed in these experiments, however the hypothesis that blocking these molecules would affect migration was specified in advance, though the direction of the effect was not predicted. We therefore analysed these experiments using a linear mixed model approach, which accounts for variation between mice and experiments as random effects in addition to our fixed effects (movement parameters). These experiments suggested a role for LFA-1 in accumulation and migration, which we tested by co-transferring LFA-1 deficient and wild type cells to mice and measuring migration and accumulation by intra-vital microscopy and flow cytometry. In these experiments the hypothesis was specified in advance. Randomization and blinding could not be performed in these experiments as both the experimental and control groups were contained in the same mouse.

Having identified LFA-1 as a likely candidate for T cell migration and residence in the liver we performed a series of controlled laboratory experiments to investigate this further (Figures 2-7). In these experiments at least 4 mice per group were used in each individual experiment where the *n* was determined by the number of mice. Data presented are typically pooled from multiple experiments, and were therefore usually analysed using linear mixed models, which account for variation due to random effects (individual mice and

experiments). Data from all mice studied are presented in the figures and no outliers were excluded. In these experiments the hypotheses were specified in advance. No randomization or blinding was performed, however in many experiments control and experimental groups (cells) were contained within the same animal.

Mice

C57BL/6.J mice, *Rag1*$^{-/-}$ mice, OT-I mice (37), *B2m*$^{-/-}$ mice (38) and uGFP mice (39) were bred in house at ANU. mTmG mice (40) were purchased from Jackson laboratories and maintained at the ANU. ITGAL C77F (*Itgal*$^{I/-}$) mice were identified in our ongoing ENU mutagenesis screens (22). ITGAL-C77F mice were maintained on a C57BL/6.J background and crossed to an OT-I uGFP background as required. All animal procedures were approved by the Animal Experimentation Ethics Committee of the Australian National University (Protocol numbers: A2013/12; A2014/62 and A2015/76).

Immunizations

Mice were immunized i.v. with 5×10^4 *P. berghei* CS^{5M} sporozoites expressing mCherry (23) dissected by hand from the salivary glands of *Anopheles stephensi* mosquitoes. Mice were then treated with 0.6mg choloroquine i.p daily for 10 days to prevent the development of blood stage infection. LCMV-Armstrong was delivered i.p. at a dose of 2×10^5 pfu/mouse.

Antibody blockade

The following antibodies were injected i.v. 2 hours prior to transfer of activated OT-I CD8$^+$T cells: anti-ICAM-1 (clone YN1/1.7.4; BioXCell; 50 μg/mouse (18)); anti-VCAM-1 (clone 429; Biolegend; 50 μg/mouse (16)) anti-CD44 (clone KM81, blocking CD44 binding to hyaluronan; Cedarlane; 20 μg/mouse (14)), Rat IgG2b isotype control (clone LTF2; BioXCell; 50 μg/mouse).

Multi-photon microscopy

Mice were prepared for multi-photon microscopy essentially as described in the supplementary experimental procedures (41). Imaging was performed using a Fluoview FVMPE-RS multiphoton microscope system (Olympus) equipped with a XLPLN25XWMP2 objective (25×; NA1.05; water immersion; 2mm working distance). Images were acquired using FV30 software (Olympus) and exported to Imaris (Bitplane) for downstream processing as described in the supplementary experimental procedures. Movies were annotated and prepared for display using Adobe After Effects (Adobe).

Statistical analysis

Details of statistical analysis for each experiment is given in the relevant figure legend. χ^2 tests, t tests, Mann-Whitney U tests and one-way ANOVAs were performed using Prism6 (GraphPad). Where data were pooled from multiple experiments, multi-level analyses were performed using a linear mixed model (LMM) in GenStat (VSNi). LMMs are a regression analysis model containing both fixed and random effects: fixed effects being the variable/treatment under examination, whilst random effects are unintended factors that may

influence the variable being measured. If significance was found from running a LMM, pair-wise comparisons of the least significant differences of means (LSD) was undertaken to determine at which level interactions were occurring. Statistical significance was assumed if the p-value was < 0.05 for a tested difference. (ns = not significant, *= $p < 0.5$, ** = $p < 0.01$, *** = $p < 0.001$, **** = $p < 0.0001$).

Supplementary Material

Refer to Web version on PubMed Central for supplementary material.

Acknowledgments

We thank Michael Devoy, Harpreet Vohra and Catherine Gillespie of the Imaging and Cytometry Facility at the John Curtin School of Medical Research for assistance with flow cytometry and multi-photon microscopy. We also thank Theresa Neeman of the ANU statistical consulting unit for assistance with statistical analysis of the data and Professor Dale Godfrey (University of Melbourne) for reagents and advice in the initial identification of the *Itgal* mutant mice.

Funding: This work was supported by startup funds from the Australian National University (to IAC) and grants from the Perpetual Foundation (IAC, FR2014/1152) and Ian Potter Foundation (IAC, Grant #32616), the Ramaciotti Foundation (CG and AE), the National Institutes of Health (CGG, U19 AI100627) and the National Health and Medical Research Council (AE, GNT1035858).

References and Notes

1. Sallusto F, Lenig D, Forster R, Lipp M, Lanzavecchia A. Two subsets of memory T lymphocytes with distinct homing potentials and effector functions. Nature. 1999; 401:708. [PubMed: 10537110]
2. Gebhardt T, et al. Memory T cells in nonlymphoid tissue that provide enhanced local immunity during infection with herpes simplex virus. Nature immunology. 2009; 10:524. [PubMed: 19305395]
3. Masopust D, et al. Dynamic T cell migration program provides resident memory within intestinal epithelium. The Journal of experimental medicine. 2010; 207:553. [PubMed: 20156972]
4. Masopust D, Vezys V, Wherry EJ, Barber DL, Ahmed R. Cutting edge: gut microenvironment promotes differentiation of a unique memory CD8 T cell population. J Immunol. 2006; 176:2079. [PubMed: 16455963]
5. Steinert EM, et al. Quantifying Memory CD8 T Cells Reveals Regionalization of Immunosurveillance. Cell. 2015; 161:737. [PubMed: 25957682]
6. Wakim LM, Gupta N, Mintern JD, Villadangos JA. Enhanced survival of lung tissue-resident memory CD8(+) T cells during infection with influenza virus due to selective expression of IFITM3. Nature immunology. 2013; 14:238. [PubMed: 23354485]
7. Gebhardt T, et al. Different patterns of peripheral migration by memory CD4+ and CD8+ T cells. Nature. 2011; 477:216. [PubMed: 21841802]
8. Schenkel JM, et al. T cell memory. Resident memory CD8 T cells trigger protective innate and adaptive immune responses. Science. 2014; 346:98. [PubMed: 25170049]
9. Fernandez-Ruiz D, et al. Liver-Resident Memory CD8+ T Cells Form a Front-Line Defense against Malaria Liver-Stage Infection. Immunity. 2016; 45:889. [PubMed: 27692609]
10. Mackay LK, et al. Hobit and Blimp1 instruct a universal transcriptional program of tissue residency in lymphocytes. Science. 2016; 352:459. [PubMed: 27102484]
11. Crispe IN, Dao T, Klugewitz K, Mehal WZ, Metz DP. The liver as a site of T-cell apoptosis: graveyard, or killing field? Immunological reviews. 2000; 174:47. [PubMed: 10807506]
12. Keating R, et al. Virus-specific CD8+ T cells in the liver: armed and ready to kill. J Immunol. 2007; 178:2737. [PubMed: 17312116]
13. Mackay LK, et al. The developmental pathway for CD103(+)CD8+ tissue-resident memory T cells of skin. Nature immunology. 2013; 14:1294. [PubMed: 24162776]

14. Guidotti LG, et al. Immunosurveillance of the liver by intravascular effector CD8(+) T cells. Cell. 2015; 161:486. [PubMed: 25892224]
15. Bertolino P, et al. Early intrahepatic antigen-specific retention of naive CD8+ T cells is predominantly ICAM-1/LFA-1 dependent in mice. Hepatology. 2005; 42:1063. [PubMed: 16250049]
16. John B, Crispe IN. Passive and active mechanisms trap activated CD8+ T cells in the liver. J Immunol. 2004; 172:5222. [PubMed: 15100260]
17. Ohteki T, Maki C, Koyasu S, Mak TW, Ohashi PS. Cutting edge: LFA-1 is required for liver NK1.1+TCR alpha beta+ cell development: evidence that liver NK1.1+TCR alpha beta+ cells originate from multiple pathways. J Immunol. 1999; 162:3753. [PubMed: 10201888]
18. Thomas SY, et al. PLZF induces an intravascular surveillance program mediated by long-lived LFA-1-ICAM-1 interactions. The Journal of experimental medicine. 2011; 208:1179. [PubMed: 21624939]
19. Cockburn IA, et al. In vivo imaging of CD8+ T cell-mediated elimination of malaria liver stages. Proceedings of the National Academy of Sciences of the United States of America. 2013; 110:9090. [PubMed: 23674673]
20. Warren A, et al. T lymphocytes interact with hepatocytes through fenestrations in murine liver sinusoidal endothelial cells. Hepatology. 2006; 44:1182. [PubMed: 17058232]
21. Smith A, Bracke M, Leitinger B, Porter JC, Hogg N. LFA-1-induced T cell migration on ICAM-1 involves regulation of MLCK-mediated attachment and ROCK-dependent detachment. Journal of cell science. 2003; 116:3123. [PubMed: 12799414]
22. Cook MC, Vinuesa CG, Goodnow CC. ENU-mutagenesis: insight into immune function and pathology. Current opinion in immunology. 2006; 18:627. [PubMed: 16889948]
23. Cockburn IA, Tse SW, Zavala F. CD8+ T cells eliminate liver stage Plasmodium parasites without detectable bystander effect. Infection and immunity. 2014
24. Laidlaw BJ, et al. CD4+ T cell help guides formation of CD103+ lung-resident memory CD8+ T cells during influenza viral infection. Immunity. 2014; 41:633. [PubMed: 25308332]
25. Anderson KG, et al. Cutting edge: intravascular staining redefines lung CD8 T cell responses. J Immunol. 2012; 189:2702. [PubMed: 22896631]
26. Slutter B, et al. Dynamics of influenza-induced lung-resident memory T cells underlie waning heterosubtypic immunity. Science Immunology. 2017; 2:eaag2031.
27. Masopust D, Vezys V, Marzo AL, Lefrancois L. Preferential localization of effector memory cells in nonlymphoid tissue. Science. 2001; 291:2413. [PubMed: 11264538]
28. Bose TO, et al. CD11a regulates effector CD8 T cell differentiation and central memory development in response to infection with Listeria monocytogenes. Infection and immunity. 2013; 81:1140. [PubMed: 23357382]
29. Casey KA, et al. Antigen-independent differentiation and maintenance of effector-like resident memory T cells in tissues. J Immunol. 2012; 188:4866. [PubMed: 22504644]
30. Mackay LK, et al. T-box Transcription Factors Combine with the Cytokines TGF-beta and IL-15 to Control Tissue-Resident Memory T Cell Fate. Immunity. 2015; 43:1101. [PubMed: 26682984]
31. Boutet M, et al. TGFbeta Signaling Intersects with CD103 Integrin Signaling to Promote T-Lymphocyte Accumulation and Antitumor Activity in the Lung Tumor Microenvironment. Cancer research. 2016; 76:1757. [PubMed: 26921343]
32. Sela U, et al. The inhibition of autoreactive T cell functions by a peptide based on the CDR1 of an anti-DNA autoantibody is via TGF-beta-mediated suppression of LFA-1 and CD44 expression and function. J Immunol. 2005; 175:7255. [PubMed: 16301630]
33. Mehal WZ, Juedes AE, Crispe IN. Selective retention of activated CD8+ T cells by the normal liver. J Immunol. 1999; 163:3202. [PubMed: 10477588]
34. Thatte J, Dabak V, Williams MB, Braciale TJ, Ley K. LFA-1 is required for retention of effector CD8 T cells in mouse lungs. Blood. 2003; 101:4916. [PubMed: 12623847]
35. Ely KH, Cookenham T, Roberts AD, Woodland DL. Memory T cell populations in the lung airways are maintained by continual recruitment. J Immunol. 2006; 176:537. [PubMed: 16365448]

36. MacPhee PJ, Schmidt EE, Groom AC. Intermittence of blood flow in liver sinusoids, studied by high-resolution in vivo microscopy. The American journal of physiology. 1995; 269:G692. [PubMed: 7491960]

37. Hogquist KA, et al. T cell receptor antagonist peptides induce positive selection. Cell. 1994; 76:17. [PubMed: 8287475]

38. Koller BH, Marrack P, Kappler JW, Smithies O. Normal development of mice deficient in beta 2M, MHC class I proteins, and CD8+ T cells. Science. 1990; 248:1227. [PubMed: 2112266]

39. Schaefer BC, Schaefer ML, Kappler JW, Marrack P, Kedl RM. Observation of antigen-dependent CD8+ T-cell/ dendritic cell interactions in vivo. Cellular immunology. 2001; 214:110. [PubMed: 12088410]

40. Muzumdar MD, Tasic B, Miyamichi K, Li L, Luo L. A global double-fluorescent Cre reporter mouse. Genesis. 2007; 45:593. [PubMed: 17868096]

41. van de Ven AL, Kim P, Ferrari M, Yun SH. Real-time intravital microscopy of individual nanoparticle dynamics in liver and tumors of live mice. 2013

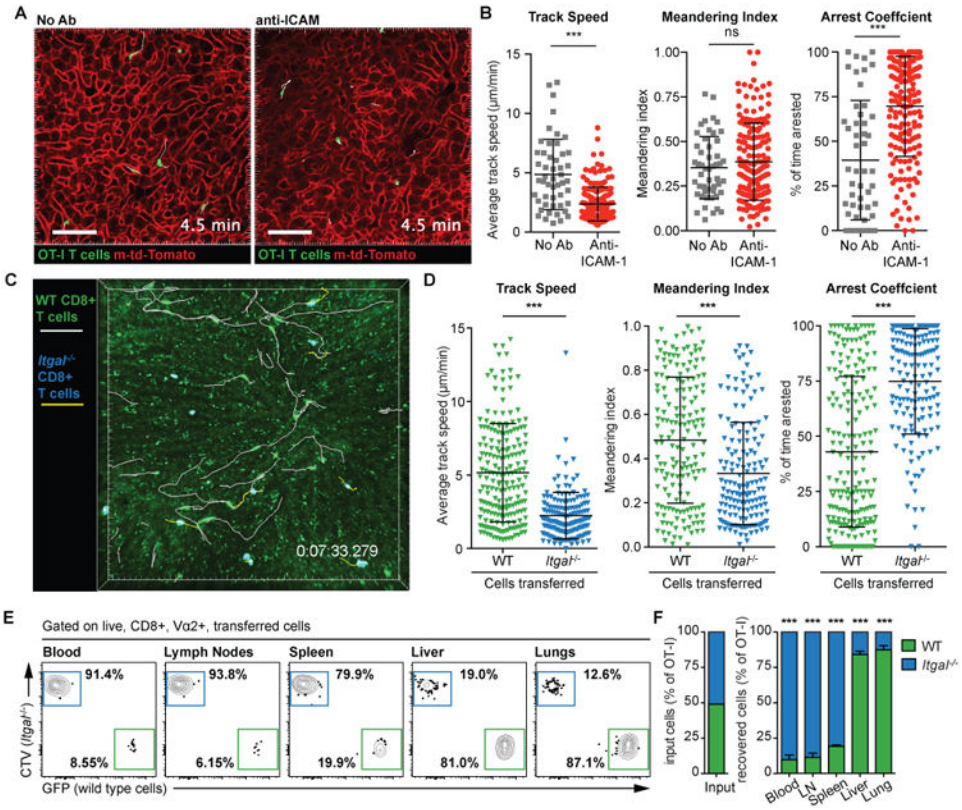

Fig 1. LFA-1:ICAM-1 interactions are required for CD8+ T cell motility in the liver

(A) 2. hours prior to the transfer of 7×10^6 in vitro activated OT-I T cells, mice (WT or mT/mG) were treated with blocking Abs to ICAM-1. 4 hours after cell transfer mice were prepared for intravital imaging and imaged by 2-photon microscopy using a standard galvanometer-scanner to acquire a 50-micron deep Z-stack approximately every 30 seconds. Representative images from time lapse imaging of mT/mG mice either with or without anti-ICAM-1 are shown. Scale bar is 30 μm. (**B**) Movement parameters of OT-I cells following anti-ICAM-1 treatment; data pooled from 4 experiments and analyzed using linear mixed models with experiment and mouse as random effects and speed, meandering index or arrest as the fixed effects. Means and standard deviations (SD) are shown. (**C**) 7×10^6 in vitro activated *Itgal*$^{-/-}$ OT-I T cells (labeled with cell trace violet) and 7×10^6 in vitro activated GFP$^+$ WT OT-I$^+$ T cells were co-transferred to WT recipient mice. Mice were imaged as in (A); image shows a representative frame from a time-lapse movie showing tracks of the *Itgal*$^{-/-}$ (yellow) and WT T cells (white); scale bar is 50 μm. (**D**) Movement parameters of *Itgal*$^{-/-}$ and WT cells in the livers of naive recipient mice as described in C; data are pooled from 3 mice in 2 independent experiments and analyzed as in (B). (**E**) 2×10^6 in vitro activated *Itgal*$^{-/-}$ OT-I CD8$^+$ T cells (labeled with cell trace violet) and 2×10^6 in vitro activated GFP$^+$ WT OT-I CD8$^+$ T cells were co-transferred to WT recipient mice. 24 hours later the blood, lymph nodes, spleen, liver and lungs were harvested and the proportion of WT and *Itgal*$^{-/-}$ cells in each organ determined by flow cytometry (representative plots all from the same mouse shown). (**F**) Summary data for the proportions of WT and *Itgal*$^{-/-}$ cells in organs harvested from 5 mice in one of two similar independent experiments, analyzed by one

sample t-test (compared to the input proportions of WT and *Itgal*$^{-/-}$ cells). Means and SD are presented.

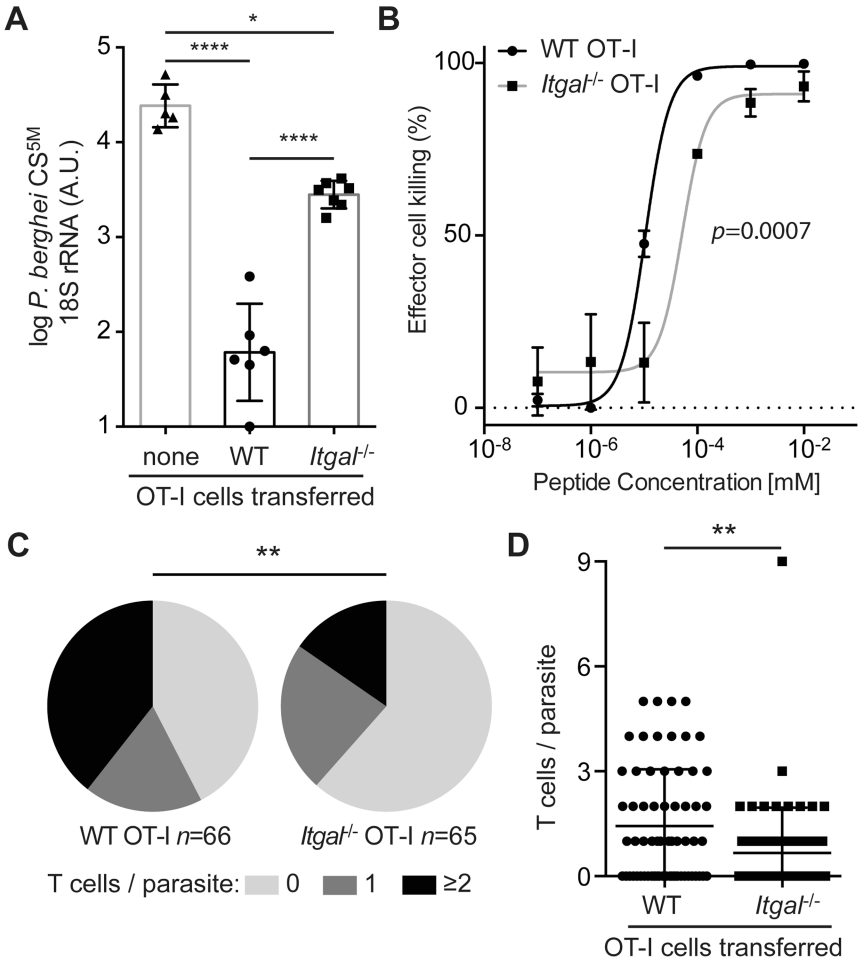

Fig 2. *Itgal* $^{-/-}$ cells do not efficiently protect against sporozoite challenge

(**A**) 2 × 10^6 *Itgal* $^{-/-}$ or littermate WT OT-I T cells were transferred to C57BL/6 mice 1 day before mice were challenged with 5 × 10^3 *P. berghei* CS^{5M} sporozoites. 24 hours post-challenge livers were harvested from the recipient mice and controls and the parasite load assessed by RT-PCR. Data are from one of 2 similar experiments with 5-7 mice/group, assessed by one-way ANOVA with Tukey's post-test for multiple comparisons. Means and SD of log transformed data are presented. (**B**) EL4 target cell killing following incubation with in vitro activated *Itgal* $^{-/-}$ or littermate *Itgal* $^{+/+}$ OT-I T cells. Data are expressed as the number of live-pulsed target cells recovered compared to the number of live-unpulsed target cells after 6 hours. Means and SD are based on 3 technical replicates, from one of two experiments, *p* value is the probability the IC_{50} values are different (extra sum-of-squares F test). (**C**) Mice were infected with 1.5 × 10^5 *P. berghei* CS^{5M}-GFP sporozoites, 15 hours later the mice received either 7 × 10^6 *Itgal* $^{-/-}$ or littermate WT OT-I T cells labeled with CTV; 20 hours post-infection mice were prepared for imaging and a 40-micron Z-slice was taken of each parasite. Pie charts show the proportion of parasites with 0, 1 and ≥2 T cells in contact analyzed by χ^2 test while (**D**) shows the number of T cells per parasite for each condition analyzed by Mann-Whitey U test. Data are from 3 mice receiving *Itgal* $^{-/-}$ cells and 4 mice receiving WT OT-I cells Bars show means and SD.

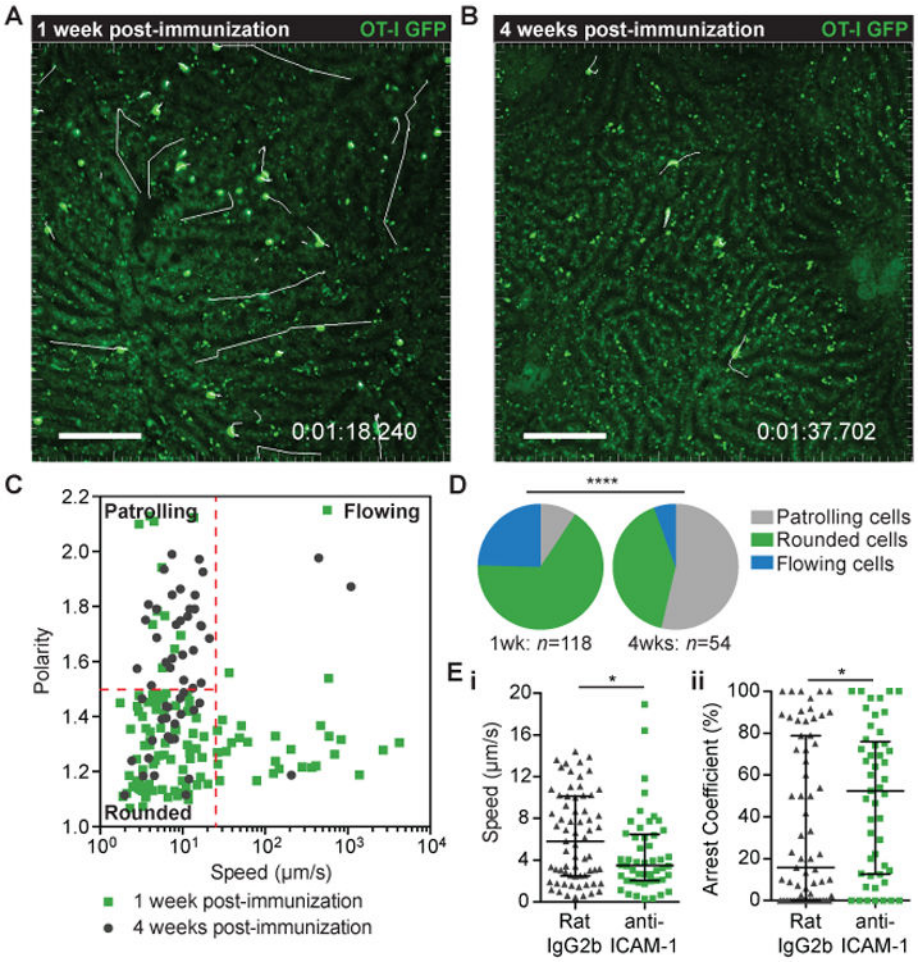

Fig 3. Memory CD8$^+$ T cells display patrolling behavior in the liver

2×10^4 GFP$^+$ OT-I cells were transferred to C57BL/6 mice prior to immunization with 5×10^4 *P.berghei* CS^{5M} sporozoites. 1 week (**A**) and 4 weeks (**B**) post-immunization mice were prepared for intra-vital imaging and the livers imaged by 2-photon microscopy using a resonant scanner to collect time-lapse moves of a single Z-slice at ~3 frames/second; images are representative time-points with T cell tracks shown in white; scale bar is 50 μm. (**C**) Mean speed vs. polarity of T cells in the liver, 1 week (green points) and 4 weeks (grey points) post-immunization. (**D**) Proportion of cells exhibiting different T cell migration behaviors 1 week and 4 weeks post immunization, analysis was performed by a χ^2 test. (**E**) (i) mean speed and (ii) arrest coefficients of OT-I GFP T cells in the liver 4 weeks post immunization (analysis based on 50um Z stacks at 1 frame/30secs). Mice received 50 μg anti-ICAM or isotype control antibodies 3 hours before imaging. Analysis was performed by one-tailed Mann-Whitney U test as the direction of the expected effect was already known from previous experiments. Data are pooled from 6 mice in each experimental group; medians and interquartile ranges are presented.

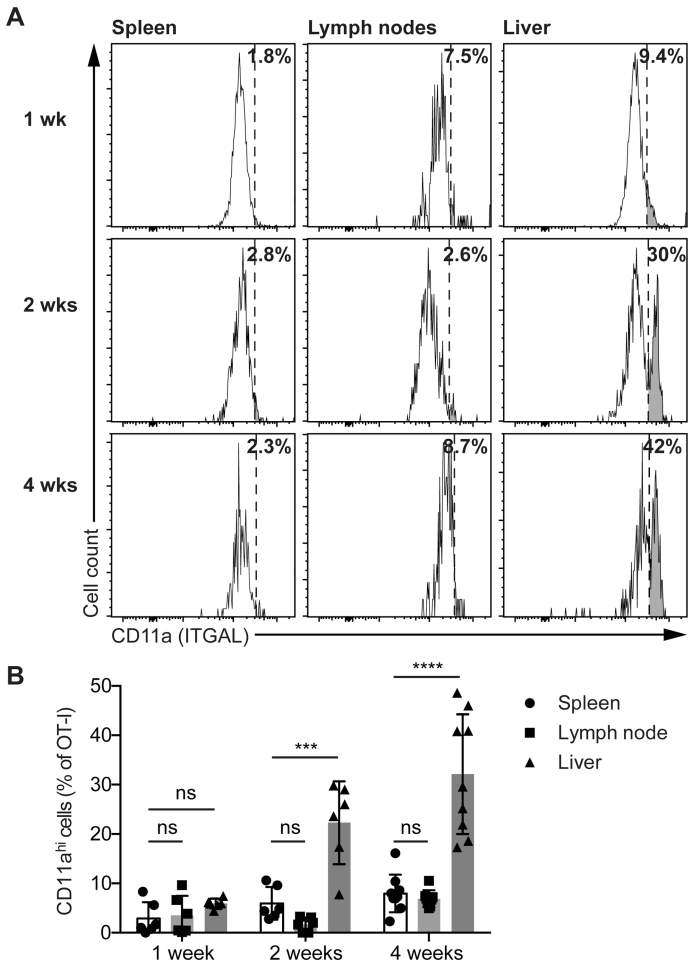

Fig 4. LFA-1 is highly expressed on a subset of liver memory CD8$^+$ T cells

2×10^4 CD45.1$^+$ OT-I cells were transferred to C57BL/6 mice prior to immunization with 5×10^4 *P.berghei* CS^{5M} sporozoites. One, 2 and 4 weeks post-immunization organs were harvested and cells prepared for flow-cytometry analysis. **(A)** Representative flow cytometry plots from a single mouse at each time-point, showing the expression of CD11a (ITGAL) on CD45.1$^+$ CD8$^+$ OT-I T cells in the spleen, lymph nodes and liver at the indicated time-points, values indicate the percentage of cells that are CD11a^{hi}. **(B)** Summary data pooled from two independent experiments showing the proportion of CD45.1$^+$ CD8$^+$ OT-I cells that are CD11a^{hi}. Data were analyzed using a linear mixed model including the experiment and mouse as random effects and organ and time-point as fixed effects. Bars show means and SD.

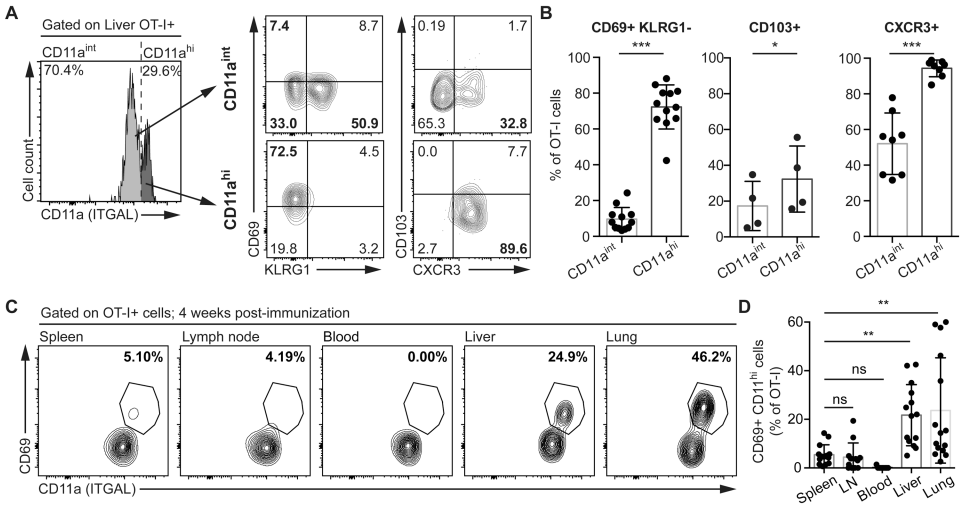

Fig 5. CD11a^{hi} memory CD8^{+} T cells in the liver have a T$_{RM}$ phenotype

2×10^4 CD45.1^{+} naïve OT-I cells were transferred to C57BL/6 mice prior to immunization with 5×10^4 *P.berghei* CS^{5M} sporozoites. (**A)** Representative flow cytometry plots of the expression of CD69, KLRG1, CD103 and CXCR3 by CD45.1^{+} CD8^{+} OT-I T cells expressing intermediate and high levels of ITGAL (CD11a^{int} and CD11a^{hi}) in the liver 4 weeks post-immunization. (**B)** Summary plots showing the proportion of cells expressing the indicated phenotypes 4 weeks post-immunization in the liver. Data are pooled from 4 independent experiments for CD69 and KLRG1, a single experiment for CD103 and 2 independent experiments for CXCR3; data were analyzed by linear mixed models including mouse as a random effect and CD11a subset as a fixed effect. Bars show means and SD. **(C)** Representative flow cytometry plots showing the co-expression of CD69 and CD11a in the indicated organs (from a single animal) 4 weeks post-immunization. (**D)** Summary of the proportion of OT-I cells in the indicated organs that are CD11a^{hi} CD69^{+}. Data are pooled from 3 independent experiments and analyzed using a linear mixed model including mouse as a random effect and the organ as the fixed effect. Bars show means and SD.

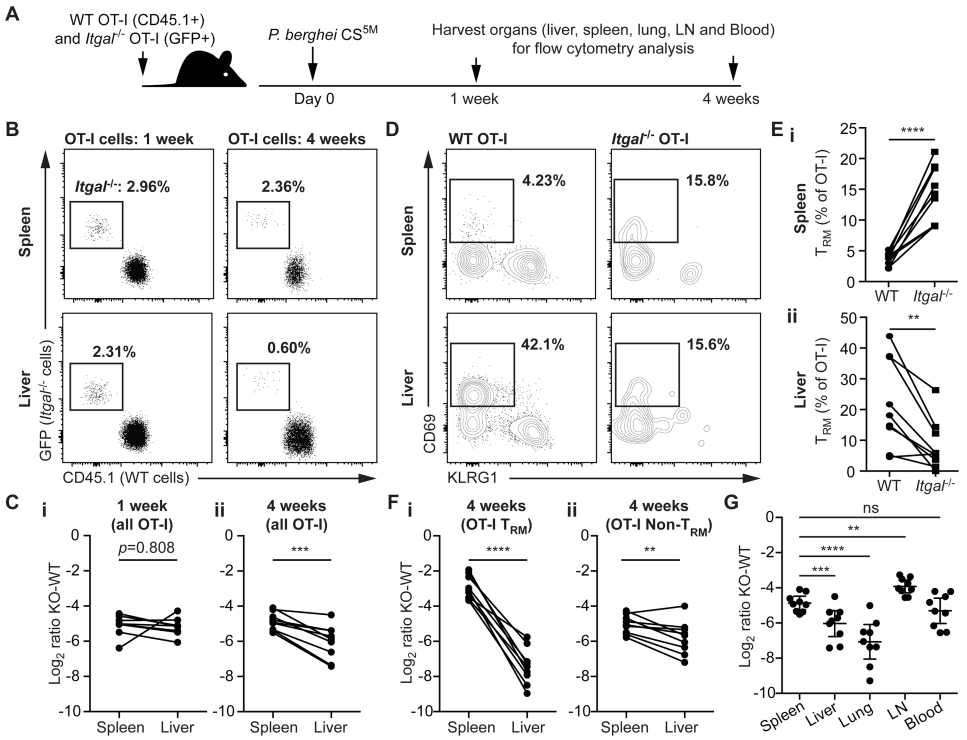

Fig 6. LFA-1 is required for residence of *Plasmodium* specific T_{RM} cells in the liver

(A) 2×10^4 naïve CD45.1$^+$ WT OT-I cells were co-transferred with 2×10^4 naïve GFP$^+$ *Itgal*$^{-/-}$ OT-I cells to C57BL/6 1 day prior to immunization with 5×10^4 *P. berghei* CS^{5M} sporozoites, at 1 week and 4 weeks post-immunization organs were harvested and the number and phenotype of transferred cells determined by flow cytometry. **(B)** Representative plots from a single mouse at each time-point showing the expansion of the different OT-I$^+$ populations in the spleen and liver 1 and 4 weeks post immunization. **(C)** Summary data showing the overall ratio of *Itgal*$^{-/-}$ (KO) to WT OT-I cells in the spleen and liver of mice (i) 1 week and (ii) 4 weeks post-immunization. **(D)** Representative flow cytometry plots showing the T_{RM} phenotype of WT and *Itgal*$^{-/-}$ OT-I cells in the spleen and liver of a single animal 4 weeks post immunization. **(E)** Summary data the showing percentage of WT and *Itgal*$^{-/-}$ OT-1 cells that are T_{RM} in (i) the spleen and (ii) livers 4 weeks post immunization. **(F)** Summary data showing the overall ratio of *Itgal*-/- (KO) to WT OT-I cells that are (i) T_{RM} and (ii) non T_{RM}. **(G)** Summary data of the overall ratio of *Itgal*$^{-/-}$ (KO) to WT OT-I cells in different organs of mice analyzed 4 weeks post-immunization; bars show means and SD. All data are pooled from 9 mice in 2 independent experiments. Panels C and F were analyzed using linear mixed models with mouse as a random effect and organ as the fixed effect. Panel E was analyzed similarly to C but with genotype as the fixed effect. Panel G was analyzed similarly to C but with experiment included as a random effect.

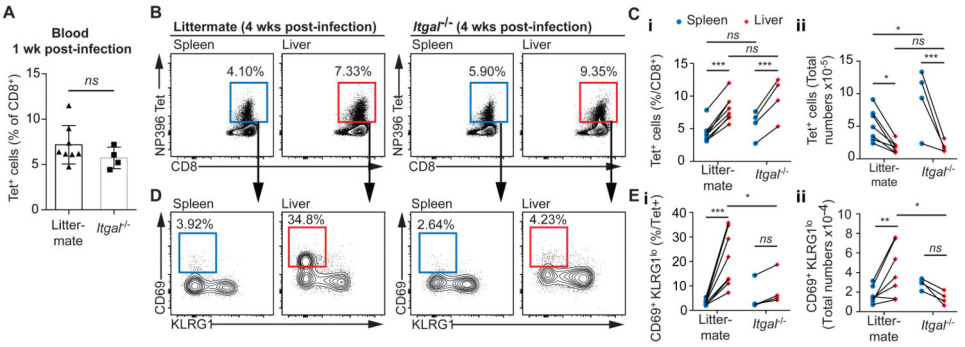

Fig 7. *Itgal*$^{-/-}$ mice do not form liver T_{RM}s following LCMV infection

Itgal$^{-/-}$ and littermate mice were infected with 2 × 10^5 pfu/mouse LCMV Armstrong. (**A**) 1 week post-infection the % of $CD8^+$ T cells in the blood that was NP396-specific was measured by flow cytometry; data are mean and SD analyzed using a 2-tailed students t-test. 4 weeks post-infection the NP396 specific immune response was measured in the spleen and liver by flow cytometry, with (**B**) representative flow cytometry plots from individual mice and (**C**) summary data presented. We further determined the proportion of antigen specific cells that had the T_{RM} phenotype ($CD69^+$ $KLRG1^{lo}$) by flow cytometry for each organ and genotype, with (**D**) representative flow cytometry plots from individual mice and (**E**) summary data presented. Data in B-E were analyzed using linear mixed models including mouse as a random effect and organ and genotype and fixed effects; pairwise *p* values derived from the models are given.